# Equations-of-motion method: Potential energy curves for $N_2$, CO, and $C_2H_4$*

William Coughran, John Rose, Tai-Ichi Shibuya†, and Vincent McKoy

*Arthur Amos Noyes Laboratory of Chemical Physics,* § *California Institute of Technology, Pasadena, California 91109*

(Received 14 September 1972)

We have applied the equations-of-motion method to various states of $N_2$, CO, and ethylene at nuclear configurations slightly distorted from the ground equilibrium geometry. This approach attempts to calculate energy differences instead of absolute energies and is thus relatively insensitive to the accuracy of the assumed ground state wavefunction. By using the experimental behavior of the ground state on distortion, we can generate accurate potential energy curves for the excited states in the region of spectroscopic interest. These curves confirm the spectroscopic behavior of the $^1\Sigma_u^+$ states of $N_2$ and the $^1\Sigma^+$ states of CO where valence and Rydberg states of the same symmetry interact. The results for the $T$ and $V$ states of ethylene agree with experiment and show that the $V$ state is predominantly a highly correlated valence state. Oscillator strengths across an absorption band are also accurately determined in this method. We report the dependence of the transition moment on bond length for the $X\,^1\Sigma^+ \rightarrow A\,^1\Pi$ transition in CO, which is in excellent agreement with experiment.

## I. INTRODUCTION

We have discussed the equations-of-motion method as an approach specifically designed to predict the spectroscopic and response properties of atoms and molecules directly.[1,2] By concentrating efforts on the direct calculation of the observables of physical interest, e.g., excitation frequencies, transition moments, and differential cross sections, one can avoid many of the difficulties involved in obtaining highly accurate wavefunctions for various states of the system in order to predict these relative quantities. In the equations-of-motion method, one calculates a set of amplitudes for each excited state that are actually components of the transition density between that state and the ground state. These amplitudes and excitation frequencies, which are the eigenfunctions and eigenvalues of a matrix, are the solution of the equations of motion.

Recently we presented results of calculations on many excited states of $N_2$, CO, and $C_2H_4$.[2] These calculations were all done at the equilibrium geometry of the ground state. The resulting vertical excitation energies and transition moments were in good agreement with experiment and indicated that the equations-of-motion method is a practical and accurate approach to predicting these spectroscopic quantities. In this paper we show that the equations of motion (EOM) can be used to obtain potential energy curves and electronic transition moments at the corresponding internuclear geometries. The approach is straightforward. Our proposed solution of the equations-of-motion is restricted to atoms and molecules with closed-shell ground states and therefore the Hartree–Fock (HF) ground state is a single Slater determinant and the particle-hole vacuum. Moreover, in the expansion of the ground state wavefunction, $|0\rangle$, with explicit two-particle correlations,[3] i.e.,

$$|0\rangle = |\mathrm{HF}\rangle + \sum_{\gamma<\delta}\sum_{m<n} C_{\gamma\delta}{}^{mn} c_m{}^{+} c_n{}^{+} c_\delta c_\gamma, \qquad (1)$$

we assume that the correlation coefficients $\{C_{\gamma\delta}{}^{mn}\}$ are small compared with unity. If these correlation coefficients become large or if $|\mathrm{HF}\rangle$ must be an open-shell wavefunction, one has to develop a different solution to the equations of motion, i.e., an open-shell theory.[4] Results on this aspect of the theory will be published in future papers.[5] However, for molecules with closed-shell ground states, we can use the present theory to obtain excitation frequencies at nuclear configurations away from equilibrium for which the correlation coefficients $\{C_{\gamma\delta}{}^{mn}\}$ do not become too large relative to unity. As the internuclear distance increases, some of these coefficients can become large so as to yield the right dissociation limit. However, we expect these coefficients to remain small enough to allow us to use the closed-shell form of our theory at geometries of practical spectroscopic interest, e.g., up to 30% change from equilibrium.

In this paper we discuss the results of calculations on several states of $N_2$, CO, and $C_2H_4$ at various internuclear distances. These results include the excitation frequencies and transition moments for eleven states of $N_2$ at six internuclear distances from $R=0.9$ to 1.40 Å and for nine states of CO at five internuclear distances from $R=0.97$ to 1.32 Å. The results are generally in good agreement with experiment. From these excitation frequencies and the experimental ground state potential energy curves, we construct potential energy curves for all the states of $N_2$ and CO. The results for the $b'\,^1\Sigma_u^+$ and $c'\,^1\Sigma_u^+$ states are of particular interest to current experimental studies. Our results are in quantitative agreement with the conclusions of Dressler[6]

and Lefebvre-Brion[7] on the locations of a valencelike $b'\,^1\Sigma_u^+$ state and a Rydberg-like $c'\,^1\Sigma_u^+$ state. The electronic transition moment of the $b'\,^1\Sigma_u^+$ state has a strong dependence on the internuclear distance. For the $X\,^1\Sigma^+ \rightarrow A\,^1\Pi$ transition in CO, we obtain a dependence of the electronic transition moment on the internuclear distance, in agreement with the measurements of Lassettre and Skerbele[8] and Zipf and co-workers.[9] It is necessary to include this dependence of the transition moment on the internuclear distance in deriving the $f$ value for this band from lifetime data. We also report results of calculations on planar ethylene in the $V$ and $T$ states and a Rydberg state at various C–C distances. Assuming a Morse potential with a dissociation energy of 6.4 eV on C–C stretching for planar ethylene in the ground state, we obtain equilibrium C–C distances in the $T$, $V$, and $R$ states of approximately 1.53, 1.7–1.8, and 1.43 Å, respectively. Calculations are also carried out for twisted ethylene at angles of twist of 30° and 45°. As in the case of $N_2$ and CO, we find that the results are generally good provided one does not go far enough from equilibrium so that the closed-shell approximation in Eq. (1) becomes invalid. Such cases become very clear in practice.

In the next section we give a very brief outline of the theory and the equations-of-motion method. Section III gives the results of the calculations on $N_2$, CO, and ethylene.

## II. THEORY

In this section we give a brief outline of the solution of the equations of motion. References 1 and 2 contain the necessary details. It can be shown that the operator $O_\lambda^+$, which generates an excited state $|\lambda\rangle$ from the ground state is exactly a solution of the equation,[10]

$$\langle 0 \,|\, [\delta O_\lambda, H, O_\lambda^+] \,|\, 0\rangle = \omega_\lambda \langle 0 \,|\, [\delta O_\lambda, O_\lambda^+] \,|\, 0\rangle \quad (2)$$

for all variations $\delta O_\lambda$. The double commutator is defined by

$$2[A, H, B] = [A, [H, B]] + [[A, H], B] \quad (3)$$

and $\omega_\lambda$ is the excitation energy $E_\lambda - E_0$. If $O_\lambda^+$ is restricted to single particle-hole form, one obtains the following equation for the amplitudes in $O_\lambda^+$ and the excitation frequency $\omega_\lambda$,

$$\begin{bmatrix} \mathbf{A} & \mathbf{B} \\ -\mathbf{B}^* & -\mathbf{A}^* \end{bmatrix} \begin{bmatrix} Y(\lambda) \\ Z(\lambda) \end{bmatrix} = \omega_\lambda \begin{bmatrix} D & 0 \\ 0 & D \end{bmatrix} \begin{bmatrix} Y(\lambda) \\ Z(\lambda) \end{bmatrix}, \quad (4)$$

where the elements of $\mathbf{A}$ and $\mathbf{B}$ are ground state expectation values of double commutators of the Hamiltonian and particle-hole operators. We refer to Refs. 1 and 2 for the defining equations for the matrix elements appearing in Eq. (4). The most relevant aspect here is that our solution of Eq. (4) assumes the ground state of the system is a closed shell and hence the two-particle correlation coefficients are small compared with unity in Eq. (1), and the single determinant $|\,\mathrm{HF}\rangle$ is the main component of the exact wavefunction $|\,0\rangle$. For the stretching of diatomic and simple polyatomic molecules, we expect these conditions to be satisfied for internuclear distances up to about 30% away from the equilibrium value. In most cases the excitation energies from the equations of motion as a function of internuclear distance, along with the ground state potential energy curve should yield potential energy curves of the excited states in this region. We can also determine the variation of the electronic transition moment across a band from the excitation amplitudes.[9]

In the following sections we discuss the results of calculations on various states of $N_2$, CO, and $C_2H_4$ at several internuclear distances. As in our previous calculations at the ground state geometry,[2] we include both single particle–hole and two particle–hole operators in the excitation operator $O_\lambda^+$. These two approximations are referred to as the $(1p\text{–}1h)$ and $(1p\text{–}1h)+(2p\text{–}2h)$ theories, respectively. We have recently discussed the inclusion of two particle–hole states in the solution of the equations of motion showing explicitly that the theory, including two particle–hole components, is equivalent to a renormalized single particle–hole theory.[11]

## III. APPLICATIONS

### A. States of $N_2$

The electron configuration of the ground state of $N_2$ is

$$(1\sigma_g)^2(1\sigma_u)^2(2\sigma_g)^2(2\sigma_u)^2(\pi_u)^4(3\sigma_g)^2.$$

We have solved for the excitation frequencies and transition moments at six internuclear distances, $R=0.90$, 1.00, 1.094($R_e$), 1.20, 1.30, and 1.40 Å, for the following eleven states: $B\,^3\Pi_g$, and $a\,^1\Pi_g(3\sigma_g \rightarrow \pi_g)$, $A\,^3\Sigma_u^+$, $b'\,^1\Sigma_u^+$, $B\,^3\Sigma_u^-$, $a'\,^1\Sigma_u^-$, $W\,^3\Delta_u$, and $w\,^1\Delta_u(\pi_u \rightarrow \pi_g)$, $c'\,^1\Sigma_u^+(3\sigma_g \rightarrow 3\sigma_u)$, $C\,^3\Pi_u$, and $b\,^1\Pi_u(2\sigma_u \rightarrow \pi_g)$. We indicate in parentheses the principal excitation in each state.

After a Hartree–Fock calculation at each internuclear distance, the equations of motion are first solved in the $1p\text{–}1h$ approximation including all particle-hole pairs of the appropriate symmetry except those of the very low $1\sigma_g$ and $1\sigma_u$ hole levels and the very high particle levels. The basis set is that of Ref. 2 and contains both valence Gaussian functions $[4s3p]$ contracted from a $(9s5p)$ primitive set and two diffuse $d\pi$ functions and two diffuse $p\sigma$ functions at the center of the molecule. We then include the effects of two particle-hole components $(2p\text{–}2h)$ on the excitation energies and consistently renormalize the oscillator strengths.

Table I lists the excitation energies for the eleven states of $N_2$ at six internuclear distances. The agreement with experiment is quite good. The excitation

TABLE I. Excitation energies[a]: States of $N_2$.

| $X\,^1\Sigma_g^+\rightarrow$ | $B\,^3\Pi_g$ | | | $a\,^1\Pi_g$ | | |
|---|---|---|---|---|---|---|
| $R$ (Å) | $(1p\text{–}1h)$ | $(1p\text{–}1h)+(2p\text{–}2h)$ | Obs[b] | $(1p\text{–}1h)$ | $(1p\text{–}1h)+(2p\text{–}2h)$ | Obs |
| 0.90 | 12.7 | 11.0 | ... | 14.6 | 12.3 | ... |
| 1.00 | 10.9 | 9.0 | 9.4 | 12.9 | 10.3 | 10.5 |
| 1.094[c] | 9.6 | 7.5 | 8.1 | 11.5 | 8.8 | 9.3 |
| 1.20 | 8.2 | 5.9 | 6.8 | 10.0 | 7.2 | 8.0 |
| 1.30 | 7.1 | 4.8 | 5.8 | 8.9 | 6.1 | 7.0 |
| 1.40 | 6.3 | 4.0 | 4.9 | 8.0 | 5.3 | 6.0 |
| | | $A\,^3\Sigma_u^+$ | | | $B'\,^3\Sigma_u^-$ | |
| 0.90 | 13.2 | 12.7 | ... | 15.9 | 15.1 | ... |
| 1.00 | 10.5 | 9.9 | ... | 13.3 | 12.4 | ... |
| 1.094 | 8.4 | 7.8 | 7.8 | 11.3 | 10.2 | 9.7 |
| 1.20 | 6.4 | 5.7 | 5.9 | 9.3 | 8.1 | 7.8 |
| 1.30 | 5.1 | 4.2 | 4.4 | 7.9 | 6.6 | 6.4 |
| 1.40 | 4.0 | 3.2 | 3.2 | 6.7 | 5.4 | 5.3 |
| | | $W\,^3\Delta_u$ | | | $a'\,^1\Sigma_u^-$ | |
| 0.90 | 14.8 | 14.3 | ... | 15.9 | 15.4 | ... |
| 1.00 | 12.1 | 11.5 | ... | 13.3 | 12.7 | ... |
| 1.094 | 10.1 | 9.4 | 8.9 | 11.3 | 10.6 | 9.9 |
| 1.20 | 8.1 | 7.3 | 7.1 | 9.3 | 8.5 | 8.1 |
| 1.30 | 6.7 | 5.8 | 5.6 | 7.9 | 6.9 | 6.6 |
| 1.40 | 5.5 | 4.7 | 4.5 | 6.7 | 5.8 | 5.5 |
| | | $W\,^1\Delta_u$ | | | $b'\,^1\Sigma_u^+$ | |
| 0.9 | 16.5 | 15.7 | ... | 19.6 | 17.9 | ... |
| 1.0 | 14.0 | 13.0 | ... | 18.3 | 16.6 | ... |
| 1.094 | 12.0 | 11.0 | 10.3 | 16.8 | 15.0 | 14.4 |
| 1.20 | 10.0 | 9.0 | 8.5 | 15.0 | 13.2 | 12.8 |
| 1.30 | 8.6 | 7.3 | 7.2 | 13.1 | 11.4 | 11.2 |
| 1.40 | 7.3 | 6.0 | 6.0 | 11.0 | 9.1 | 9.7 |
| | | $c'\,^1\Sigma_u^+$ | | | $C\,^3\Pi_u$ | |
| 0.90 | 15.8 | 12.8 | ... | 14.4 | 12.5 | ... |
| 1.00 | 15.6 | 12.3 | 13.0 | 13.8 | 11.5 | ... |
| 1.094 | 15.5 | 12.1 | 12.9 | 13.3 | 10.8 | 11.1 |
| 1.20 | 15.4 | 12.0 | 12.6 | 12.9 | 10.1 | 10.6 |
| 1.30 | 15.2 | 11.6 | 12.3 | 12.7 | 9.6 | 10.0 |
| 1.40 | 14.9 | 11.5 | ... | 12.7 | 9.3 | 9.3 |
| | | $b\,^1\Pi_u$ | | | | |
| 0.90 | 17.7 | 14.9 | ... | | | |
| 1.00 | 17.6 | 14.5 | ... | | | |
| 1.094 | 17.4 | 14.0 | 13.0 | | | |
| 1.20 | 17.2 | 13.4 | 12.0 | | | |
| 1.30 | 17.3 | 12.9 | 10.7 | | | |
| 1.40 | 17.5 | 12.7 | 9.4 | | | |

[a] In electron volts.

[b] The experimental results are from W. Benesch, J. T. Vanderslice, S. G. Tilford, and P. G. Wilkinson, Astrophys. J. **142**, 1227 (1965) and J. Geiger and B. Schroeder, J. Chem. Phys. **50**, 7 (1969).

[c] Experimental equilibrium internuclear distance.

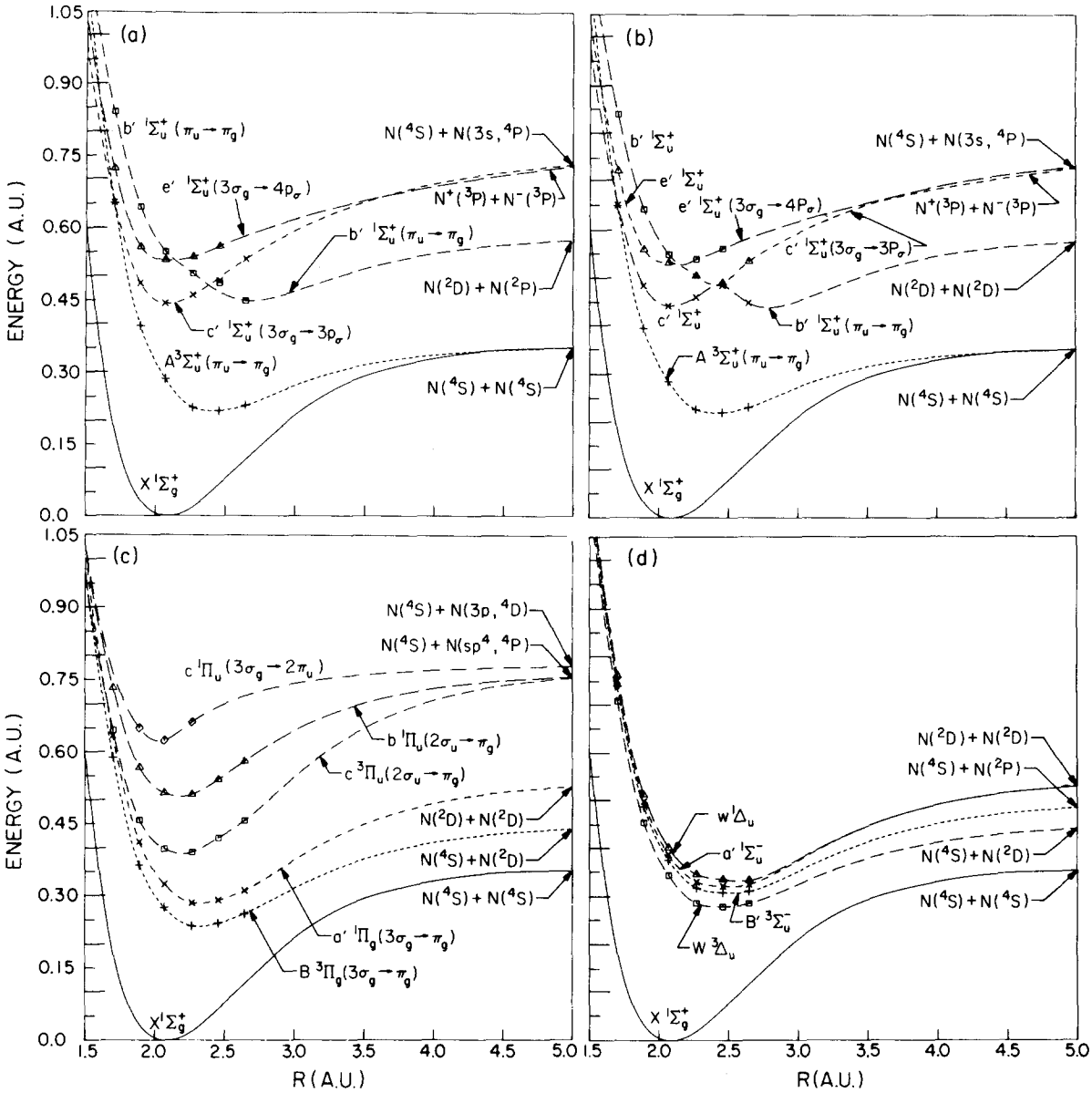


FIG. 1. Potential energy curves for the excited states of $N_2$. The basis set is $[4s3p]+R(2p\sigma, 2d\pi)$ (see text). The ground state curve is taken from F. Gilmore, J. Quant. Spectrosc. Radiat. Transfer **5**, 369 (1965). (a) "Deperturbed" representation of the $\Sigma_u^+$ states. (b) Adiabatic $\Sigma_u^+$ states utilizing the noncrossing rule. (c) $\Pi_u$ and $\Pi_g$ states. (d) $\Delta_u$ and $\Sigma_u^-$ states (all $\pi_u \rightarrow \pi_g$).

frequencies in the $(1p\text{–}1h)$ approximation are all larger than the observed values but the inclusion of $2p\text{–}2h$ components leads to a decrease in these excitation energies and excitation frequencies in fairly good agreement with experiment. We do not want to make any extensive comparisons between these results and those derived by other methods, since our main purpose is to test the practicality and accuracy of our method and to see how well it does in describing closed-shell systems away from equilibrium geometry. The results of calculations at internuclear distances beyond $R=1.4$ become poorer and show that the closed-shell assumption in our theory[2] is beginning to fail at these distances. Some correlation coefficients become as large as 0.3–0.4 at these distances. Fortunately this occurs at distances that are already large for practical spectroscopic interests.

Figure 1(a)–(d) shows plots of the potential energy curves for these states of $N_2$ that are derived from these frequencies and the experimental ground state potential energy curve. These derived curves agree quite well with the observed potential energy curves, e.g., the minima are all close to the observed values. Of special interest here are the states labeled $b'\,{}^1\Sigma_u^+$ and $c'\,{}^1\Sigma_u^+$.[12] Dressler[6] has shown that the observed ${}^1\Sigma_u^+$ states in the 12.4–14.3 eV region of the spectrum

TABLE II. Oscillator strengths for transitions in $N_2$.[a]

| | $X\,^1\Sigma_g^+ \rightarrow b\,^1\Pi_u$ | | $X\,^1\Sigma_g^+ \rightarrow b'\,^1\Sigma_u^+$ | | $X\,^1\Sigma_g^+ \rightarrow c'\,^1\Sigma_u^+$ | |
|---|---|---|---|---|---|---|
| $R$ (Å) | $(1p\text{–}1h)$ | $(1p\text{–}1h)+(2p\text{–}2h)$[b] | $(1p\text{–}1h)$ | $(1p\text{–}1h)+(2p\text{–}2h)$[b] | $(1p\text{–}1h)$ | $(1p\text{–}1h)+(2p\text{–}2h)$[b] |
| 0.90 | 0.58 | 0.46 | 0.13 | 0.11 | 0.07 | 0.05 |
| 1.00 | 0.62 | 0.48 | 0.13 | 0.11 | 0.09 | 0.07 |
| 1.094 | 0.64 | 0.46 | 0.49 | 0.42 | 0.11 | 0.08 |
| 1.20 | 0.58 | 0.40 | 0.59 | 0.50 | 0.001[c] | 0.001 |
| 1.30 | 0.58 | 0.40 | 0.31 | 0.26 | 0.12 | 0.08 |
| 1.40 | 0.60 | 0.36 | 0.13 | 0.10 | 0.22 | 0.15 |

[a] The electronic oscillator strength $f_{el}=\frac{2}{3}G\cdot\Delta E\cdot M^2$, where $M$ is the dipole transition matrix element and $G$ the degeneracy factor.

[b] These values include the effect of a decrease in the excitation energies in going from the $(1p\text{–}1h)$ to $(1p\text{–}1h)+(2p\text{–}2h)$ approximation and a scaling of the $1p\text{–}1h$ amplitudes due to the inclusion of $2p\text{–}2h$ amplitudes.

[c] Due to an avoided crossing at around $R=1.25$ Å. See text for discussion.

can be interpreted in terms of "deperturbed" states of a valence type ($b'\,^1\Sigma_u^+$) and a Rydberg type ($c'\,^1\Sigma_u^+$). These "deperturbed" curves correspond to hypothetical electronic states of the same symmetry that are permitted to cross each other.[6] The electrostatic interaction terms between these states is expected to be small, since their electron configurations are very different and hence our calculated potential energy curves should essentially be the deperturbed curves except very close to a crossing point. In Fig. 1(a), we have drawn our curves for these states as deperturbed curves, and in Fig. 1(b) we preserve the noncrossing rule and show continuous states that assume different electron configurations with internuclear distance. Our results agree with the observations of Lefebvre-Brion[7] and Dressler,[6] i.e., the $b'\,^1\Sigma_u^+$ state is a $\pi_u\rightarrow\pi_g$ intravalence transition with $R_e\cong1.43$ Å and the $c'\,^1\Sigma_u^+$ a Rydberg $3\sigma_g\rightarrow3\sigma_u$ transition with $R_e\approx1.11$ Å. The deperturbed results give $R_e=1.45$ Å for the $b'\,^1\Sigma_u^+$ state and $R_e=1.12$ Å for the $c'\,^1\Sigma_u^+$ state. The observed $^1\Pi_u$ states can also be analyzed by assuming an interaction between a valence $b\,^1\Pi_u$ state and Rydberg states $c\,^1\Pi_u$ and $o\,^1\Pi_u$. Our calculated valence $b\,^1\Pi_u(2\sigma_u\rightarrow\pi_g)$ has an $r_e$ of about 1.16 Å, which is smaller than the value of 1.32 Å derived by Dressler.[6] This state is the least well-described of the valence excited states of $N_2$ because of the importance of double excitations ($2p\text{–}2h$ components). At $R=0.9$ Å the $\pi_g$ orbital has a second moment in the direction perpendicular to the molecular axis of 3.7 Å$^2$, and the $b\,^1\Pi_u$ state is essentially a single particle–hole state. At $R_e$ of the ground state and beyond, double excitations becomes important and the $\pi_g$ orbital is of a typical valence size. A more accurate inclusion of double excitations may be necessary to describe this state. The $c\,^1\Pi_u$ is primarily a $3\sigma_g\rightarrow3p\pi$ Rydberg state and the $o\,^1\Pi_u$ state is a $\pi_u\rightarrow3s$ Rydberg state; these states are not adequately described in this basis that contains no diffuse $p_\pi$ or $s$ functions. A $c\,^1\Pi_u$ curve is included for completeness in Fig. 1(c); it does not cross the $b\,^1\Pi_u$ state as it should to produce the strong experimental perturbation.[6]

Table II gives the electronic oscillator strengths for the $X\,^1\Sigma_g^+\rightarrow b\,^1\Pi_u$, $b'\,^1\Sigma_u$, and $c'\,^1\Sigma_u^+$ transitions at several internuclear distances.[13] These oscillator strengths do not contain any Franck–Condon factors. The behavior of the oscillator strength for the $b'\,^1\Sigma_u^+$ state is very interesting. At smaller internuclear distance, i.e., $R=0.90$ and 1.00 Å, the $f$-value is only about 0.1 but increases to 0.5–0.6 at $R=1.094$ and 1.20 Å. The reason for this is that at the smaller distances the $\pi_g$ orbital begins to acquire some Rydberg character, e.g., the orbital's second moment $\langle\pi_g\,|\,x^2+y^2\,|\,\pi_g\rangle$ is about 7.6 Å$^2$. This reflects the Rydberg-valence mixing of the hypothetical deperturbed states and perhaps the onset of united-atom behavior. At the larger internuclear distances, the state becomes more valencelike, e.g., a $\pi_g$ orbital second moment of 2.8 Å$^2$ at $R=1.22$ Å. We also see that the $X\,^1\Sigma_g^+\rightarrow c'\,^1\Sigma_u^+$ transition has an $f$-value that becomes very small at $R=1.20$ Å. This is due to the interaction of the $b'\,^1\Sigma_u^+$ and $c'\,^1\Sigma_u^+$ states whose "deperturbed" curves cross at $R=1.22$ Å.[6]

### B. States of CO

The electron configuration of the ground state of CO is

$$(1\sigma)^2(2\sigma)^2(3\sigma)^2(4\sigma)^2(1\pi)^4(5\sigma)^2.$$

We have obtained the excitation frequencies and transition moments at the five internuclear distances, $R=$ 0.98, 1.09, 1.13($R_e$), 1.21, and 1.32 Å, for these states of CO: $a\,^3\Pi$, and $A\,^1\Pi(5\sigma\rightarrow2\pi)$, $a'\,^3\Sigma^+$, $e\,^3\Sigma^-$, $I\,^1\Sigma^-$, $d\,^3\Delta$, $D\,^1\Delta$, and $^1\Sigma^+(1\pi\rightarrow2\pi)$, $B\,^1\Sigma^+(5\sigma\rightarrow3s)$, and $C\,^1\Sigma^+(5\sigma\rightarrow3p\sigma)$. The electron configuration of the principal component of each state is shown in parentheses. The basis set used in these calculations is a $[3s2p]$ set contracted from a $(7s3p)$ valence Gaussian set, plus a single $s$ and $p\sigma$ on the C and O atoms[2] representing $n=3$ atomic orbitals and single diffuse

TABLE III. Excitation energies[a]: States of CO.

| $X\,^1\Sigma^+\rightarrow$ | $a\,^3\Pi$ | | | $A\,^1\Pi$ | | |
|---|---|---|---|---|---|---|
| $R$ (Å) | $(1p\text{–}1h)$ | $(1p\text{–}1h)+(2p\text{–}2h)$ | Obs[b] | $(1p\text{–}1h)$ | $(1p\text{–}1h)+(2p\text{–}2h)$ | Obs |
| 0.97 | 8.8 | 7.4 | ... | 12.2 | 10.1 | ... |
| 1.09 | 7.6 | 6.5 | 6.6 | 11.0 | 9.1 | 8.8 |
| 1.13 | 7.2 | 6.0 | 6.1 | 10.3 | 8.5 | 8.4 |
| 1.21 | 6.6 | 5.4 | 5.6 | 9.6 | 7.6 | 7.7 |
| 1.32 | 5.7 | 4.4 | 5.0 | 8.3 | 6.1 | 6.8 |
| | | $a'\,^3\Sigma^+$ | | | $e\,^3\Sigma^-$ | |
| 0.97 | 13.1 | 11.2 | ... | 15.6 | 13.1 | ... |
| 1.09 | 10.5 | 9.1 | 9.3 | 12.9 | 11.0 | 10.8 |
| 1.13 | 9.5 | 8.1 | 8.5 | 11.9 | 10.0 | 9.8 |
| 1.21 | 8.3 | 6.6 | 7.0 | 10.6 | 8.3 | 8.2 |
| 1.32 | 6.6 | 4.5 | 5.5 | 8.8 | 6.0 | 6.6 |
| | | $d\,^3\Delta$ | | | $I\,^1\Sigma^-$ | |
| 0.97 | 14.5 | 12.4 | ... | 15.6 | 13.3 | ... |
| 1.09 | 11.8 | 10.3 | 10.1 | 12.9 | 11.2 | 10.9 |
| 1.13 | 10.9 | 9.3 | 9.2 | 11.9 | 10.2 | 9.8 |
| 1.21 | 9.6 | 7.7 | 7.7 | 10.6 | 8.5 | 8.3 |
| 1.32 | 7.8 | 5.5 | 6.1 | 8.8 | 6.2 | 6.7 |
| | | $D\,^1\Delta$ | | | $B\,^1\Sigma^+$[c] | |
| 0.97 | 16.1 | 13.5 | ... | 12.3 | 10.3 | 10.6[d] |
| 1.09 | 13.4 | 11.5 | ... | 12.9[e] | 11.0 | 10.8 |
| 1.13 | 12.5 | 10.4 | 10.5 | 12.8 | 10.9 | 10.8 |
| 1.21 | 11.1 | 8.7 | 8.4 | 13.1[e] | 11.0 | 10.8 |
| 1.32 | 9.3 | 6.3 | 6.8 | 12.9 | 10.5 | 10.8[d] |
| | | $C\,^1\Sigma^+$[c] | | | | |
| 0.97 | 13.0 | 10.9 | ... | | | |
| 1.09 | 13.5[e] | 11.4 | ... | | | |
| 1.13 | 13.5 | 11.3 | 11.4 | | | |
| 1.21 | 13.8[e] | 11.5 | ... | | | |
| 1.32 | 14.9 | 12.4 | ... | | | |

[a] In electron volts. The experimental $R_e$ is 1.13 Å.

[b] The experimental results are from G. Herzberg, T. Hugo, S. Tilford, and J. Simmons, Can. J. Phys. **48**, 3004 (1970) and V. Meyer, A. Skerbele, and E. Lassettre, J. Chem. Phys. **43**, 805 (1965).

[c] The calculated excitation energies to the $b\,^3\Sigma^+$ and $c\,^3\Sigma^+$ states, the triplet states corresponding to the $B\,^1\Sigma^+$ and $C\,^1\Sigma^+$ states, are 10.5 and 11.2 eV at $R=1.13$ Å compared to the observed values of 10.4 and 11.6 eV, respectively.

[d] Estimated from a plot of the measured values at $R=1.09$, 1.13, and 1.21 Å.

[e] The excitation energies at this point were calculated without the diffuse $p\sigma$ function at the center of charge. This results in excitation frequencies too high by about 0.1 and 0.2 eV for the $B$ and $C$ states, respectively, but has a negligible effect on the frequencies of true valence states. See text for discussion.

$s(\zeta=0.01)$ and $p\sigma(\zeta=0.0085)$ Rydberg functions at the center of charge. The calculations at $R=1.09$ and 1.21 Å were done without the diffuse $p\sigma$ function. This hardly affects the excitation energies but we will see that the oscillator strengths for the $X\,^1\Sigma^+\rightarrow{}^1\Sigma^+$ transitions can depend quite strongly on the composition of the basis.

Table III shows the excitation energies for nine states at five internuclear distances. The agreement with experiment is quite good. We have also calculated the excitation frequencies at $R=1.43$ Å. At this internuclear distance, the predicted excitation energies are all about 0.7–1.0 eV smaller than the observed values. This is primarily due to inadequacies in the orbital

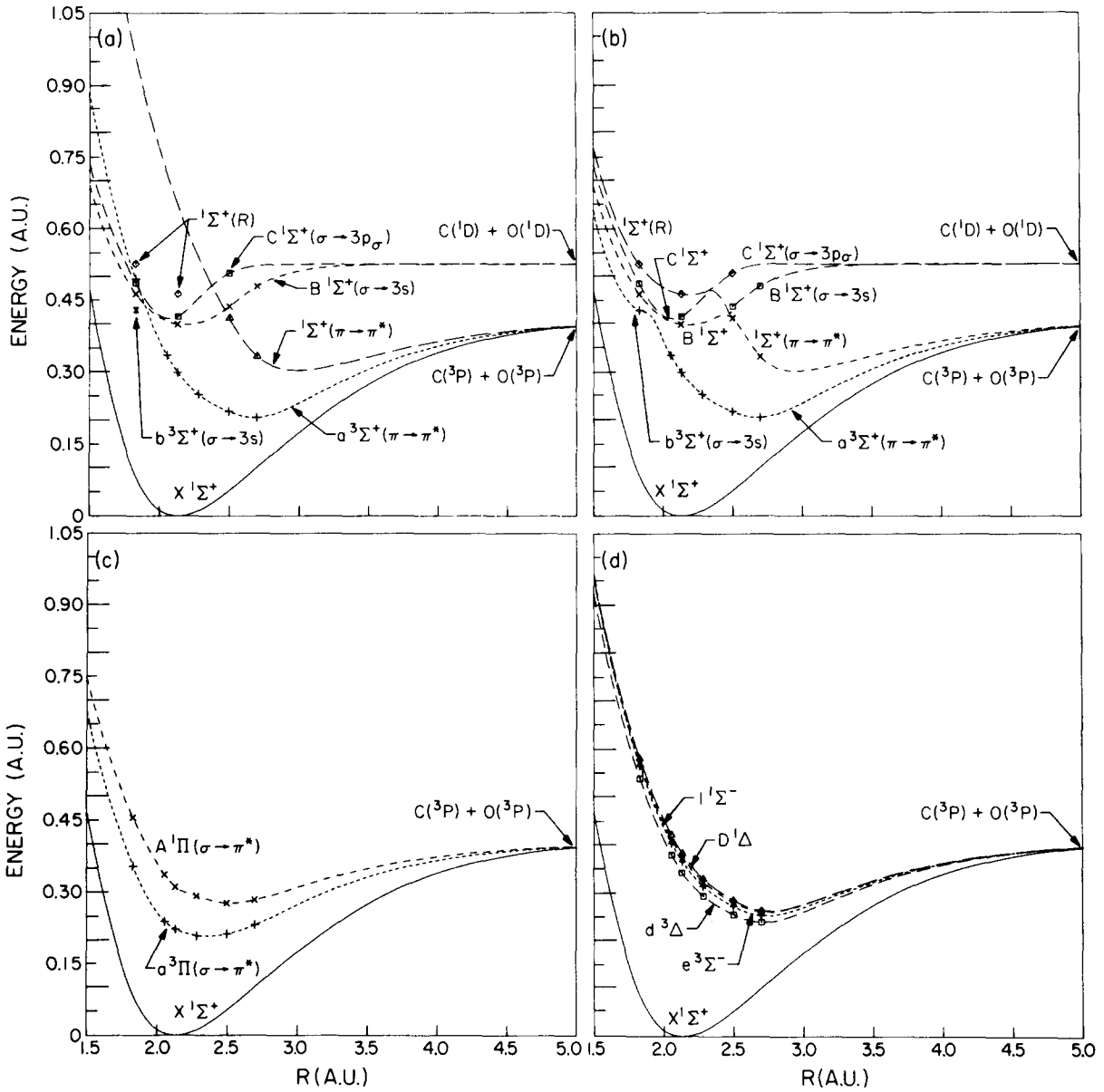


FIG. 2. Potential energy curves for the excited states of CO. The basis set is $[4s2p\pi 3p\sigma]+R(s, p\sigma)$ (see text). The ground state curve is taken from Ref. 16. (a) "Deperturbed" representation of the $\Sigma^+$ states. (b) Adiabatic representation of the $\Sigma^+$ states utilizing the noncrossing rule. (c) $\Pi$ states. (d) $\Delta$ and $\Sigma^-$ states (all $\pi\rightarrow\pi^*$).

basis since, at this internuclear distance, the correlation coefficients are small enough for the closed-shell assumption to be valid. Of special interest are the results for the $I\,^1\Sigma^-$ state, which are all within 2–7% of the observed values reported by Herzberg *et al.*[14] These results are quite different from those deduced by Krupenie and Weissman,[15] who give the excitation energies at $R=0.97$ and 1.09 Å as 7.8 and 9.1 eV. Our results therefore suggest that the experimental potential energy curve of Ref. 14 is the correct one for $R<1.09$ Å.

As in the results for $N_2$, we have used the calculated excitation energies and the experimental potential energy curve for the ground state to construct potential energy curves for the various states of CO in Fig. 2(a)–(d). These curves all agree well with experiment. Of special interest are the curves for the $^1\Sigma^+$ states. Figure 2(a) shows these potential curves for four $^1\Sigma^+$ states, i.e., $B\,^1\Sigma^+(5\sigma\rightarrow 3s)$, $C\,^1\Sigma^+(5\sigma\rightarrow 3p\sigma)$, $^1\Sigma^+(R)$, and at a few points, $^1\Sigma^+(1\pi\rightarrow 2\pi)$, a valence state. In this figure we draw these curves to correspond to approximate "deperturbed" curves that are therefore shown as crossing one another.[6] Two points are shown for the $^1\Sigma^+(R)$ state, which probably corresponds to the $E\,^1\Sigma^+$ Rydberg state observed at 11.5 eV,[16] but cannot be adequately described in the present orbital basis, especially at larger internuclear distances where

TABLE IV. Oscillator strengths for transitions in CO.[a]

| | $X\,^1\Sigma^+ \rightarrow A\,^1\Pi$ | | $X\,^1\Sigma^+ \rightarrow B\,^1\Sigma^+$ [c] | | $X\,^1\Sigma^+ \rightarrow C\,^1\Sigma^+$ [c] | |
|---|---|---|---|---|---|---|
| $R$(Å) | $(1p\text{–}1h)$ | $(1p\text{–}1h)+(2p\text{–}2h)$ [b] | $(1p\text{–}1h)$ | $(1p\text{–}1h)+(2p\text{–}2h)$ | $(1p\text{–}1h)$ | $(1p\text{–}1h)+(2p\text{–}2h)$ [b] |
| 0.97 | 0.34 | 0.28 | 0.03 | 0.03 | 0.04 | 0.03 |
| 1.09 | 0.22 | 0.18 | ... | ... | ... | ... |
| 1.13 | 0.18 | 0.14 | 0.04 | 0.03 | 0.06 | 0.04 |
| 1.21 | 0.14 | 0.10 | ... | ... | ... | ... |
| 1.32 | 0.06 | 0.04 | 0.06 | 0.04 | 0.06 | 0.05 |

[a] The electronic oscillator strength $f_{el}=\frac{2}{3}\cdot G\cdot\Delta E\cdot M^2$, where $M$ is the dipole transition matrix element and $G$ the degeneracy factor.
[b] See Footnote b of Table II.
[c] The oscillator strengths for the $B\,^1\Sigma^+$ and $C\,^1\Sigma^+$ states are strongly affected by the diffuse components of the orbital basis. We only report values for the most complete and balanced basis. See text for discussion.

it cannot retain its Rydberg character. Our calculations also predict a $^1\Sigma^+$ state that is valencelike with $1\pi\rightarrow 2\pi$ as the principal component of the excitation. This state may play a role in the $\Sigma^+$ spectrum of CO in this region, similar to that of the $b'\,^1\Sigma_u^+$ state of $N_2$. The predissociation of the $v'=2$ level of the $B\,^1\Sigma^+$ state is probably due to the $a'\,^3\Sigma^+$ to some extent,[16] but the location of this $^1\Sigma^+(1\pi\rightarrow 2\pi)$ state relative to the $B\,^1\Sigma^+$ suggests that some predissociation may take place through this mechanism. The variation of the lifetime with vibrational quantum number[17] for $v'=0$ and 1 vibrational levels of the $B\,^1\Sigma^+$ state may also be due to perturbations between these two states. In Fig. 2(b) we preserve the noncrossing rule and show continuous potential energy curves for these states. Our calculated excitation energies for the $b\,^3\Sigma^+$ and $c\,^3\Sigma^+$ states are 10.5 and 11.2 eV at $R_e$ of the ground state. These values agree well with experiment, i.e., 10.4 and 11.6 eV, respectively, and are not listed in Table II. As shown in Fig. 2, the $b\,^3\Sigma^+$ state crosses the $a\,^3\Sigma^+$ and has a lower energy at small internuclear distances.

In Table IV we give the oscillator strengths for the $X\,^1\Sigma^+\rightarrow A\,^1\Pi$, $B\,^1\Sigma^+$, and $C\,^1\Sigma^+$ transitions at the various internuclear distances. From the electron energy loss spectra, Lassettre and Skerbele[8] have obtained the dependence of the electronic transition moment on internuclear distance for the $X\,^1\Sigma^+\rightarrow A\,^1\Pi$ (Fourth Positive) band. It is now known that it is necessary to include this variation of the transition moment with $R$ to remove the discrepancy that existed between total $f$ values derived from lifetime data and electron energy loss spectra.[9] In Table V we show our calculated values of the transition moment, $\langle X\,^1\Sigma^+ \mid \sum_i \mathbf{r}_i \mid A\,^1\Pi\rangle$, at five internuclear distances. In the second column of this table, we also list the experimental values[8] for $M(R)$ at $R\approx 1.09$ and 1.13 Å, which are the two values that lie in our range of $R$. The agreement between the calculated transition moment and the experimental values is good. Figure 3 shows a plot of $M(R)$ along with a plot of Lassettre's data.[18]

The calculated $f$-values for the $X\,^1\Sigma^+\rightarrow B\,^1\Sigma^+$ and $C\,^1\Sigma^+$ transitions can be sensitive to the basis set used in the calculation. This is due to the fact that they are Rydberg-like states. For example, the $f$ values obtained in the more complete calculation of Ref. 2 are 0.05 and 0.12 for the $B$ and $C$ states, respectively, at $R=1.13$ Å. There we used a $[5s4p\sigma, 3p\pi]$ basis. This $f$ value of 0.12 for the $X\rightarrow C$ transition, although in better agreement with the observed value of 0.16,

TABLE V. Dependence of the transition moment on internuclear distance in the fourth positive band of CO.

| $R$ (Å) | $M(R)$ [a] | $M_{obs}$ [b] |
|---|---|---|
| 0.97 | 0.753 | |
| 1.09 | 0.636 | 0.59 |
| 1.13 | 0.580 | 0.56 |
| 1.21 | 0.518 | |
| 1.32 | 0.365 | |

[a] In atomic units. These values of $M(R)$ are derived from the $(1p\text{–}1h)+(2p\text{–}2h)$ values of $f$ in Table IV.
[b] These two values of Ref. 6 lie within our range of $R$. See Fig. 3 for a plot of the other data.

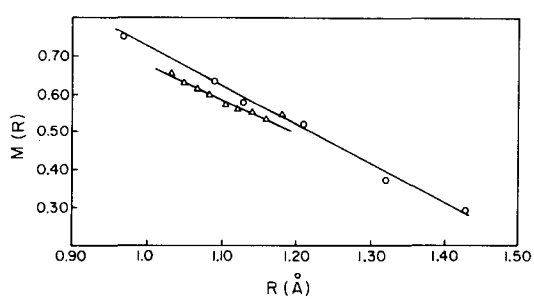


FIG. 3. Transition moment $M(R)$ vs internuclear distance for the fourth positive band of CO. $M(R)$ is in atomic units and $R$ in angstroms. The ○ points are the calculated points and the △ points are the experimental values of Ref. 8.

TABLE VI. Excitation energies: states of $C_2H_4$ as a function of C–C bond distance.[a]

| $N\rightarrow$ | $T(^3B_{3u})$[b] | | $V(^1B_{3u})$ | | $R'''(^1B_{3u})$[d] | |
|---|---|---|---|---|---|---|
| $R_{C-C}$ (Å) | $(1p\text{–}1h)$ | $(1p\text{–}1h)+(2p\text{–}2h)$ | $(1p\text{–}1h)$ | $(1p\text{–}1h)+(2p\text{–}2h)$ | $(1p\text{–}1h)$ | $(1p\text{–}1h)+(2p\text{–}2h)$ |
| 1.24 | 6.1 | 5.5 | 10.9 | 9.8 | 12.7 | 11.1 |
| 1.35[c] | 4.8 | 4.0 | 9.7 | 8.2 | 12.0 | 10.6 |
| 1.46 | 3.7 | 3.0 | 8.6 | 7.5 | 11.4 | 10.1 |
| 1.57 | 2.9 | 2.1 | 7.6 | 6.3 | 11.1 | 9.8 |
| 1.69 | 2.1 | 1.3 | 6.5 | 5.0 | 10.8 | 9.5 |
| 1.80 | 1.5 | 0.5 | 5.5 | 3.8 | 10.5 | 9.3 |

[a] Calculations are all done at a C–H bond length of 1.07 Å and a CH–CH bond angle of 120° and in the planar geometry.
[b] Excitation energies in electron volts.
[c] $R_e$ of the ground state. See Ref. 2 for a comparison of the calculated and experimental results at $R_e$.
[d] The first member of the Rydberg series of the same symmetry as the $V$ state.

would probably be lowered if more diffuse Rydberg-like functions are added to the basis.

### C. States of Ethylene

Tables VI–VIII show the results of calculations on the $N\rightarrow T(^3B_{3u})$, $N\rightarrow V(^1B_{3u})$, and $N\rightarrow R'''(^1B_{3u})$ transitions in ethylene. The $T$ and $V$ states are the triplet and singlet $\pi\rightarrow\pi^*$ states and $R'''$ is the first member of the $\pi\rightarrow nd\pi$ Rydberg series. This Rydberg state is of the same symmetry as the $V$ state. In Ref. 2 we gave results of calculations on these same states with a large basis, i.e., $[4s3p/2s]+R(3p_{zC})$ Gaussian basis, but only at the ground state equilibrium geometry. These new results with a $[3s2p/1s]$ basis contracted from the $(7s3p/3s)$ primitive set and two diffuse $p_\pi$ functions ($\zeta=0.03$ and 0.01) show the dependence of the excitation frequencies and oscillator strengths of these transitions on internuclear geometry.

TABLE VII. Oscillator strengths for the $N\rightarrow V$ transition at several C–C distances.[a]

| $R$ (Å) | $(1p\text{–}1h)$[b] | $(1p\text{–}1h)+(2p\text{–}2h)$ |
|---|---|---|
| 1.24 | 0.44 | 0.34 |
| 1.35[c] | 0.40 | 0.33 |
| 1.46 | 0.33 | 0.28 |
| 1.57 | 0.24 | 0.20 |
| 1.69 | 0.15 | 0.11 |
| 1.80 | 0.10 | 0.07 |

[a] For planar ethylene with a C–H bond length of 1.07 Å and a CH–CH bond angle of 120°.
[b] $f_{el}=\frac{2}{3}\cdot\Delta E\cdot M^2$, where $M$ is the transition moment. No Franck–Condon factors are included in this table.
[c] $R_e$ of the ground state. See Ref. 2 for a comparison with experimental results.

Table VI gives the excitation frequencies of these transitions at six C–C internuclear distances for the planar molecule. The results at $R=1.35$, $R_e$ of the ground state, can be compared with the experimental vertical excitation energies of 4.6, 7.6, and 9.0 eV, respectively.[19] The results of Ref. 2 are in better agreement with experiment especially for the $N\rightarrow R'''$ transition where we obtained an excitation frequency of 8.9 eV. However the excitation energies in this basis for this transition should give a reasonable potential energy curve but shifted to higher energies. One of our purposes is to obtain potential energy curves for planar ethylene in the $T$, $V$, and $R'''$ states. To obtain these curves, we assume a Morse curve for the C–C stretching in the ground state with $R_e=1.35$ Å, $\omega=1600$ cm$^{-1}$, and $D_e\approx 146$ kcal/mole. From this ground state potential energy curve and the excitation frequencies of Table VI, we obtain the potential energy curves for the $T$, $V$, and $R$ states shown in Fig. 4(a). The $V$ state is drawn with a dissociation limit of 8 eV.[20] These curves give C–C bond lengths in these states in agreement with the suggested experimental values.[19] The curves are approximate but reasonable changes in the dissociation limits will not change them drastically. The $T$ state has an $R_e$ of about 1.55 Å while the $V$ state has a minimum around 1.7–1.8 Å. Merer and Mulliken[19] suggest values of 1.58 and 1.8 Å for $R_e$ of the $T$ and $V$ states, respectively. The inflection point in the $V$ state at about 1.4 Å is probably a manifestation of the ionic minimum since the second moment of the $\pi^*$ orbital $\langle\pi^*\,|\,z^2\,|\,\pi^*\rangle$ is about 7 a.u.$^2$ in the region giving the state some Rydberg character. A similar inflection is seen for the $b'\,^1\Sigma_u^+$ state of $N_2$ [Fig. 1(a)]. At larger internuclear distances, the $V$ state becomes clearly valencelike with a second moment of 3–4 a.u.$^2$ The divergence of the results from the expected curve at around 1.8 Å is probably due to the large correlation coefficients appearing in the ground state wavefunction. Here $\sigma\rightarrow\sigma^*$ contributions to the $V$ state become very

TABLE VIII. Excitation energies: states of $C_2H_4$ at several torsional angles.[a]

| $N\rightarrow$ | $T(^3B_{3u})$[c] | | $V(^1B_{3u})$[c] | | $R'''(^1B_{3u})$ | |
|---|---|---|---|---|---|---|
| $\theta$[b] | $(1p\text{–}1h)$ | $(1p\text{–}1h)+(2p\text{–}2h)$ | $(1p\text{–}1h)$ | $(1p\text{–}1h)+(2p\text{–}2h)$ | $(1p\text{–}1h)$ | $(1p\text{–}1h)+(2p\text{–}2h)$ |
| 0° | 4.8 | 4.0 | 9.7 | 8.2 | 12.0 | 10.6 |
| 30° | 3.9 | 3.4 | 8.0 | 7.1 | 9.7 | 8.4 |
| 45° | 2.9 | 2.3 | 6.6 | 5.7 | 9.2 | 7.9 |

[a] With a C–H bond length of 1.07 Å and a CH–CH bond angle of 120° and $R_{C-C}=1.35$ Å.
[b] The calculations at 30° and 45° were done in a $[3s2p/1s]$ contracted valence plus two $p_y$ and $p_z$ diffuse Gaussian basis.
[c] See text for a comparison with available experimental data.

large. The points shown in Fig. 4(a) for 1.9 Å utilize correlation coefficients estimated from perturbation theory, since the equations can no longer be iterated to self-consistency at this distance; they thus only show the trend of the curves at large distances. The potential energy curve for the $R'''$ state has a minimum at around $R=1.42$ Å, which agrees well with the value of 1.41 Å observed for most Rydberg states of ethylene.[21] The $b_{2g}$ (or $\pi^*$) orbital has a second moment in the direction perpendicular to the molecular plane of 18.5 Å$^2$ in the $R'''$ state distinguishing it from the $N\rightarrow V$ transition, which is clearly an intravalence transition. Finally, we list the oscillator strengths for the $N\rightarrow V$ transition at several internuclear distances in Table VII. The $f$-value of 0.33 for the vertical transition at the ground state $R_e$ is close to the suggested total $f$ value of $N\rightarrow V$ band. The basis set used in these calculations is not adequate to describe the $f$ value of the $N\rightarrow R'''$ transition at larger C–C distances.

Table VIII lists excitation energies at torsional angles of 30° and 45° for $N\rightarrow T$, $V$, and $R'''$ transitions. In these calculations the C–C distance is kept at 1.35 Å. Calculations at 60° showed that some ground state correlation coefficients become large and hence we could not make the closed-shell assumption for the ground state wavefunction. An open-shell version of the equations-of-motion method would have to be used[4,5] to extend the calculations far enough to obtain accurate potential barriers. Estimates for the $T$ and $V$ state barriers of 1 and 3 eV from these calculations do not agree well with the observed barrier of about 2 eV. Calculations would have to be done at larger angles of twist to improve this estimate. In Fig. 4(b) we plot potential energy curves for these states from the calcu-

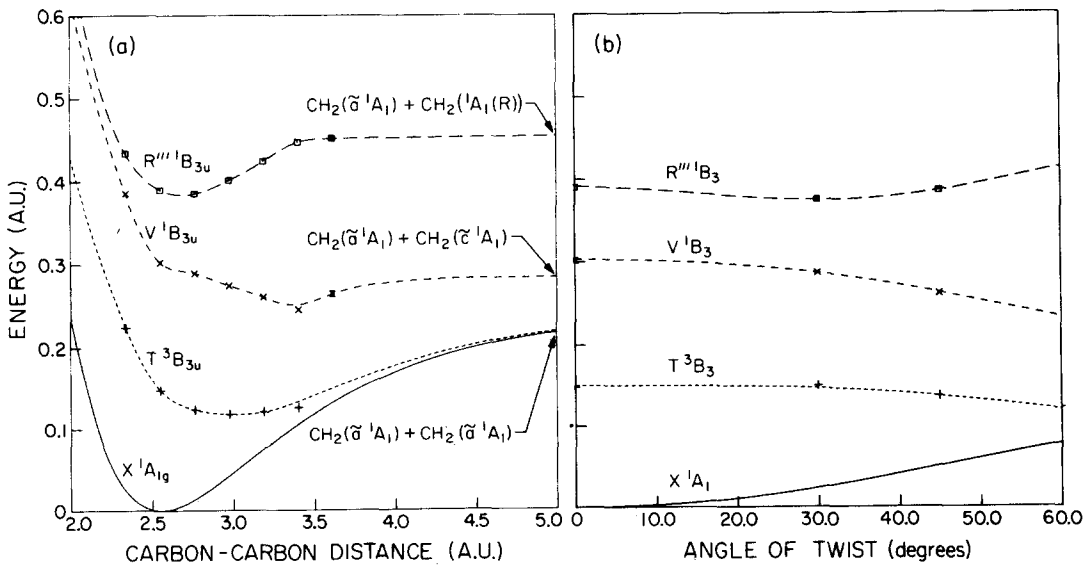


FIG. 4. Potential energy curves for the excited states of $C_2H_4$. The basis set is $[3s2p/s]+R(2p_{sC})$ (see text). (a) $B_{3u}$ states as a function of carbon–carbon bond length. The ground state curve is a Morse potential ($V=6.43\{1-\exp[-2.455(R-1.35)]\}^2$, where $V$ is in eV and $R$ in Å). (b) $B_3$ states as a function of twisting about the carbon–carbon bond. The ground state curve is taken as $V=2.3\sin^2\theta+1.3\sin^4\theta-0.8\sin^6\theta$. This fits the CI data of U. Kaldor and I. Shavitt, J. Chem. Phys. **48**, 191 (1968) for small displacements and matches the experimental barrier of 2.8 eV [B. S. Rabinovitch and F. S. Loony, J. Chem. Phys. **23**, 315 (1955)].

lated excitation energies and the suggested potential energy curve for torsion in the ground state. To compare our calculated frequencies with experiment, we assume the potential energy curves of the $V$ and $T$ states given in Ref. 19 but shifted so as to give the observed excitation energies of 7.6 and 4.6 eV at $\theta=0°$ for the $V$ and $T$ states, respectively. Our calculated frequencies agree well with these suggested experimental results. At twisting angles $\theta=0°$, 30°, and 45°, the calculated values for the $N\rightarrow T$ transition are 4.0, 3.4, and 2.3 eV, respectively, and the available experimental data suggest[19] values of 4.6, 3.2, and 1.9 eV. The nonmonotonic behavior of the curves at small angles is probably due to differences in the basis sets (diffuse $p_y$ functions are included for the twisted case). For the $N\rightarrow V$ transition we obtain values of 8.2, 7.1, and 5.7 eV at $\theta=0°$, 30°, and 45° compared with the probable experimental values of 7.6, 6.4, and 5.0 eV, respectively. The curve for the $R'''$ state shows a minimum at a torsional angle of about 30° in agreement with the observed minima at an angle of 25° in other Rydberg states and the $^3B_{1u}$ positive ion of ethylene.[19] This state is not the lowest Rydberg state of this symmetry in twisted ethylene since a $B_{3g}$ Rydberg state in planar ethylene has equivalent symmetry when the molecule is twisted. The oscillator strength for the $N\rightarrow V$ transition decreases from a value of 0.33 at $\theta=0°$ to 0.08 at 45°. From the orbital second moments, the electron density is obviously becoming less diffuse in both the $V$ and $R'''$ states as the molecule is twisted.

## IV. CONCLUSIONS

We have used the equations-of-motion method to study the excitation frequencies and transition moments for many states of $N_2$, CO, and $C_2H_4$. In this approach one calculates directly the excitation energies and transition densities as opposed to deriving these quantities by solving Schroedinger's equation separately for the absolute energies and wavefunctions of the states. The results are generally in good agreement with available experimental data. Of particular interest are the results on the $^1\Sigma_u^+$ states of $N_2$ where we predict a valencelike $b'\,^1\Sigma_u^+$ state and a Rydberg-like $c'\,^1\Sigma_u^+$ state with excitation energies and equilibrium bond distances close to the derived experimental results of Dressler[6] and Lefebvre-Brion.[7] The equations-of-motion should also predict oscillator strengths reliably and, as an example of this, we obtain a dependence of the electronic transition moment on the internuclear distance in the $X\,^1\Sigma^+\rightarrow A\,^1\Pi$ transition of CO in agreement with the measured values.[8,9] Our results and experience indicate that this approach can predict the quantities of spectroscopic interest reliably and economically.

*Work supported by the National Science Foundation.
†Present address: Department of Physics, University of the Pacific, Stockton, California 95204.
‡Alfred P. Sloan Foundation Fellow.
§Contribution No. 4551.
[1]T. Shibuya and V. McKoy, Phys. Rev. A **2**, 2208 (1970).
[2]J. Rose, T. Shibuya, and V. McKoy, J. Chem. Phys. **58**, 74 (1973).
[3]See Ref. 1 for details.
[4]D. J. Rowe and S. S. M. Wong, Nucl. Phys. A. **153**, 561 (1970).
[5]D. L. Yeager and V. McKoy (unpublished results).
[6]K. Dressler, Can. J. Phys. **47**, 547 (1969).
[7]H. Lefebvre-Brion, Can. J. Phys. **47**, 541 (1969).
[8]E. N. Lassettre and A. Skerbele, J. Chem. Phys. **54**, 1597 (1971).
[9]M. J. Mumma, E. J. Stone, and E. C. Zipf, J. Chem. Phys. **54**, 2627 (1971).
[10]D. J. Rowe, Rev. Mod. Phys. **40**, 153 (1968).
[11]T. Shibuya, J. Rose, and V. McKoy, J. Chem. Phys. (to be published).
[12]The $e'\,^1\Sigma_u^+$ state is poorly described in the present atomic orbital basis but is included in Fig. 1, since there is an avoided crossing between this state and the $b'\,^1\Sigma_u^+$ state is at about $R=2.1$ a.u. and an energy of 14.8 eV. This agrees well with the crossing of the deperturbed curves deduced from experiment. See J. Geiger and B. Schroeder, J. Chem. Phys. **50**, 7 (1969).
[13]See Ref. 2 for a comparison of our calculated $f$ values at $R_e$ of the ground state with available experimental data.
[14]G. Herzberg, T. Hugo, S. Tilford, and J. Simmons, Can. J. Phys. **48**, 3004 (1970).
[15]P. H. Krupenie and S. Weissman, J. Chem. Phys. **43**, 1529 (1965).
[16]P. H. Krupenie, Natl. Stand. Ref. Data Ser. **5**, ,(1966).
[17]R. E. Imhof and F. H. Read, *Abstracts of papers of the Seventh International Conference on the Physics of Electronic and Atomic Collisions*, July 1971 (North-Holland, Amsterdam, 1971), p. 862.
[18]In Ref. 8, $M(R)$ is actually plotted against the $r$ centroid. In this range the $r$ centroid is quite close to the $R$ value itself.
[19]See, for example, A. J. Mercer and R. S. Mulliken, Chem. Rev. **69**, 639 (1969).
[20]E. Miron, B. Raz, and J. Jortner, J. Chem. Phys. **56**, 5265 (1972).
[21]P. G. Wilkinson, Can. J. Phys. **34**, 643 (1956).